NEUROSCIENCE
RESEARCH ARTICLE
V. Jokinen et al. / Neuroscience 375 (2018) 10–24

Differential Spinal and Supraspinal Activation of Glia in a Rat Model of Morphine Tolerance

Viljami Jokinen,[a]* Yulia Sidorova,[b] Hanna Viisanen,[a] Ilida Suleymanova,[b] Henna Tiilikainen,[a] Zhilin Li,[c] Tuomas O. Lilius,[a] Kert Mätlik,[d] Jenni E. Anttila,[e] Mikko Airavaara,[e] Li Tian,[c,f] Pekka V. Rauhala[a] and Eija A. Kalso[a,g]

[a] *Department of Pharmacology, Faculty of Medicine, Haartmaninkatu 8 (Biomedicum), 00014 University of Helsinki, Helsinki, Finland*

[b] *Laboratory of Molecular Neuroscience, Institute of Biotechnology, Viikinkaari 5d, 00014 University of Helsinki, Helsinki, Finland*

[c] *Neuroscience Center, Helsinki Institute of Life Science, Viikinkaari 4, 00014 University of Helsinki, Helsinki, Finland*

[d] *Program in Developmental Biology, Institute of Biotechnology, Viikinkaari 5d, 00014 University of Helsinki, Helsinki, Finland*

[e] *Institute of Biotechnology, Viikinkaari 5d, 00014 University of Helsinki, Helsinki, Finland*

[f] *Psychiatric Research Center, Beijing Huilongguan Hospital, Peking University, Beijing, China*

[g] *Division of Pain Medicine, Department of Anaesthesiology, Intensive Care and Pain Medicine, Helsinki University Hospital and University of Helsinki, Haartmaninkatu 2A, P.O. Box 140, 00029 Helsinki, Finland*

Abstract—Development of tolerance is a well known pharmacological characteristic of opioids and a major clinical problem. In addition to the known neuronal mechanisms of opioid tolerance, activation of glia has emerged as a potentially significant new mechanism. We studied activation of microglia and astrocytes in morphine tolerance and opioid-induced hyperalgesia in rats using immunohistochemistry, flow cytometry and RNA sequencing in spinal- and supraspinal regions. Chronic morphine treatment that induced tolerance and hyperalgesia also increased immunoreactivity of spinal microglia in the dorsal and ventral horns. Flow cytometry demonstrated that morphine treatment increased the proportion of M2-polarized spinal microglia, but failed to impact the number or the proportion of M1-polarized microglia. In the transcriptome of microglial cells isolated from the spinal cord (SC), morphine treatment increased transcripts related to cell activation and defense response. In the studied brain regions, no activation of microglia or astrocytes was detected by immunohistochemistry, except for a decrease in the number of microglial cells in the substantia nigra. In flow cytometry, morphine caused a decrease in the number of microglial cells in the medulla, but otherwise no change was detected for the count or the proportion of M1- and M2-polarized microglia in the medulla or sensory cortex. No evidence for the activation of glia in the brain was seen. Our results suggest that glial activation associated with opioid tolerance and opioid-induced hyperalgesia occurs mainly at the spinal level. The transcriptome data suggest that the microglial activation pattern after chronic morphine treatment has similarities with that of neuropathic pain.

Key words: flow cytometry, opioid, neuroinflammation, nociception, microglia, transcriptomics.

INTRODUCTION

Morphine and other strong opioids are widely used to treat moderate to strong acute and cancer pain (Caraceni et al., 2012). With long-term use, opioid tolerance and opioid-induced hyperalgesia (OIH) can become major problems. OIH is a paradoxical phenomenon, where opioids increase rather than alleviate pain. OIH can lead to cessation of opioid treatment and its replacement with other analgesics (Tompkins and Campbell, 2011). In recent years, the role of glia has become increasingly interesting as a possible mediator of both opioid-induced tolerance and hyperalgesia. Glia are non-neuronal cells that regulate the homeostasis of the nervous system. Microglia- or astrocyte-mediated neuroinflammation has

*Corresponding author.
E-mail addresses: viljami.jokinen@helsinki.fi (V. Jokinen), yulia.sidorova@helsinki.fi (Y. Sidorova), hanna.viisanen@helsinki.fi (H. Viisanen), ilida.suleymanova@helsinki.fi (I. Suleymanova), henna.tiilikainen@helsinki.fi (H. Tiilikainen), zhilin.li@helsinki.fi (Z. Li), tuomas.lilius@helsinki.fi (T. O. Lilius), kert.matlik@helsinki.fi (K. Mätlik), jenni.anttila@helsinki.fi (J. E. Anttila), mikko.airavaara@helsinki.fi (M. Airavaara), li.tian@helsinki.fi (L. Tian), pekka.rauhala@helsinki.fi (P. V. Rauhala), eija.kalso@helsinki.fi (E. A. Kalso).

Abbreviations: BSA, bovine serum albumin; CGRP, calcitonin gene-related peptide; DPA, dynamic plantar aesthesiometer; FPKM, fragments per kilobase of exon per million reads mapped; GFAP, glial fibrillary acidic protein; GO, gene ontology; i.p., intraperitoneal; Iba1, ionized calcium-binding adapter molecule 1; OIH, opioid induced hyperalgesia; PBS, phosphate buffered saline; RNA, ribonucleic acid; s.c., subcutaneous.

https://doi.org/10.1016/j.neuroscience.2018.01.048
0306-4522/

been shown to contribute to nociception in various preclinical pain models such as peripheral nerve injury (Cova et al., 1988; Raghavendra et al., 2003; Zhuang et al., 2006), spinal cord (SC) injury (Hains and Waxman, 2006), post-operative pain (Obata et al., 2006), and bone cancer (Zhang et al., 2005). Functional imaging techniques have also provided evidence for glial activation in the brain of chronic pain patients (Loggia et al., 2015). Opioids have also been suggested to induce neuroinflammation via glial cells in the SC (Raghavendra et al., 2002; Watkins et al., 2005; Holdridge et al., 2007; Mattioli et al., 2010). The implications of opioid-induced glial activation are not fully understood. However, opioid-induced neuroinflammation has been proposed to contribute to morphine tolerance and OIH, as blockade of glial reactivity or their pro-inflammatory products has been shown to attenuate both conditions (Grace et al., 2015).

The extent to which opioids activate glial cells and cause neuroinflammation has been only partially studied. The effects of opioids on glial activation have previously been studied mainly in the SC and in some individual brain regions by using immunohistochemistry. Recent data have suggested that nociceptors and spinal structures alone could explain opioid tolerance and OIH (Corder et al., 2017). Therefore, we assessed glial activation, not only in the spinal, but also in supraspinal regions relevant to pain processing in a rat model of morphine tolerance and hyperalgesia. In addition to using immunohistochemistry, we used flow cytometry and RNA sequencing to clarify the cellular and molecular changes.

EXPERIMENTAL PROCEDURES

Animals

Research was conducted in accordance with the guidelines of the local authorities, International Association for the Study of Pain (Zimmermann, 1983), and European Communities Council Directive of 24 November 1986. The provincial government of Southern Finland (Uudenmaan Lääninhallitus, Hämeenlinna, Finland) had approved the study protocol. Male Sprague-Dawley rats (Scanbur, Sollentuna, Sweden) weighing 200–250 g at the beginning of experiments were used. The rats were accommodated in transparent cages, in groups of four, in temperature-controlled rooms with regular diurnal light cycle. Water and standard laboratory chow were available *ad libitum*. The rats were habituated to the testing conditions during three days prior to experiments.

Drugs

Morphine hydrochloride was purchased from the University Pharmacy (Helsinki, Finland). Morphine was dissolved to 0.9% sodium chloride (saline). Morphine and its control (saline) were administered subcutaneously (s.c.) in a volume of 2 mL/kg. The morphine doses are given as free base amounts per unit of volume.

Behavioral tests

All behavioral measurements were performed in a randomized and blinded fashion. Tail flick latencies were tested with an Ugo Basile 37360 tail flick apparatus (Comerio, Italy). The rats were restrained in plastic tubes, the tail coming out of the tube. At each time point, three different points of the middle third of the tail were subjected to the light of the apparatus. The intensity of the light was adjusted to produce a baseline latency of 3.2 ± 0.6 s (n = 30). Flick of the tail terminated the infrared light and stopped the timer of the apparatus. The mean of the results was then calculated. To avoid tissue damage, the cut-off was set to 10 s. If a measurement reached the cut-off, no further tests were performed for that time point.

Mechanical thresholds were assessed using the Ugo Basile 37450 Dynamic Plantar Aesthesiometer (DPA), (Comerio, Italy). The rats were placed on a metal mesh in cubic plastic cages and habituated 10 min before testing. A dull monofilament with a diameter of 0.5 mm was applied perpendicularly to the middle of the hindpaw of the rat. The pressure was gradually increased until a rapid withdrawal or shaking of the paw occurred. The filament withdrew automatically after the reaction and the apparatus stored the threshold of the force needed to cause the reaction. Both hindpaws of each rat were tested consecutively with an interval of 1 min and the mean of the measurements was calculated. A 40-g cut-off was used.

Cold thresholds were measured with the Bioseb T2CT Cold/Hot plate apparatus (Vitrolles, France) as adapted from Allchorne et al. (2005). The temperature of the plate was set to 0 °C which the apparatus kept constant during the measurements. The rat was set free onto the apparatus plate in a transparent cylinder. The time to the first lift or stomp of the hindpaw was recorded. Lift of the paw that was involved in coordinated movement of all four limbs was excluded. A cut-off of 180 s was used.

Experimental design

The rats were administered morphine 10 mg/kg or saline twice daily for 14 days. The first injection of the day was given at 10 a.m. (morning injection) and the second at 7 p.m. (evening injection). The behavioral measurements were performed on experiment days 1, 3, 7, 10, and 13 (tail flick and DPA) and 3, 8, and 14 (cold plate). The tail flick, DPA, and cold plate tests were performed before the morning injection (approximately 12 h from the evening injection). The tail flick test was performed also one hour after the morning injection. For immunohistochemistry, flow cytometry, and transcriptomics studies, another set of rats with a similar drug administration scheme and development of morphine tolerance was used. However, staining of substance P and calcitonin gene-related peptide (CGRP) was performed from the first set of animals.

Immunohistochemistry

After completion of the behavioral studies, tissues of animals were collected and fixed with 4% PFA and embedded to paraffin blocks. Sections of 10 μm thickness were prepared from lumbar regions of the SCs (Fig. 1) and selected regions of the brain. The

brain areas for immunohistochemical staining were located and cropped according to the atlas of Paxinos and Watson (1998). Sections were probed with antibodies for Ionized calcium-binding adapter molecule 1 (Iba1) (1:1000, Cat. No. 019-19741, Wako, Richmond, VA, USA), GFAP (1:400, Cat. No. G-3893, Sigma–Aldrich, St. Louis, MO, USA), CGRP (1:10,000, Cat. No. T-4032, Peninsula Laboratories, San Carlos, CA, USA) or substance P (1:10,000, Cat. No. T-4107, Peninsula Laboratories). Bound antibodies were visualized using anti-rabbit and anti-mouse biotinylated secondary antibodies and the VECTASTAIN ABC HRP Kit (Cat. No. PK-6101, PK-4002 Vector Laboratories, Burlingame, CA, USA) as described by the manufacturer. Slides were imaged using the 3DHISTECH Scanner (3DHISTECH Ltd, Budapest, Hungary) and scanning service provided by http://www.biocenter.helsinki.fi/bi/histoscanner/index.html). Images were analyzed with Matlab R2014b software (Mathworks, Natick, MA, USA). The number of Iba1 or GFAP-positive cells was quantified using manually-set size and intensity thresholds as described previously (Penttinen et al., 2016). The number of cells was normalized to the area of analyzed tissue. Since the morphology of glial cells is changed upon activation, we also analyzed the area covered by immunopositive stainings, determined as the total number of pixels with intensity above the selected threshold and normalized to the area of analyzed tissue in pixels. For each animal and studied region, 2–4 non-consecutive sections were analyzed and results were averaged.

Flow cytometry

Rats were deeply anaesthetized with isoflurane and perfused intracardially with 100 ml phosphate buffered saline (PBS). The L4–L6 segments of the lumbar SC, medulla and primary somatosensory cortex (PSC) were then dissected. Dissected tissues were weighed, cut into tiny pieces, and gently homogenized through 70 μm cell strainers (Fisher Scientific, Waltham, MA, USA) in PBS/1% FBS. Single cell suspensions prepared from ~25 mg tissue per sample were blocked with 5% normal rat serum, and stained with a combination of anti-rat flow cytometric markers, including Granulocyte-FITC (clone HIS48, eBioscience, San Diego, CA, USA), CD172a-PE (clone OX41, BioLegend, San Diego CA, USA), MHCII-PerCP-eFluor 710 (clone OX17, eBioscience), and CD11b/c-eFluor 660 (clone OX42, eBioscience) with light protection at 4 °C for 60-min with continuous rotation. After washing, cells were resuspended into 2 ml PBS/1% FBS/0.02% NaN_3 buffer, and acquired on a 2-laser, 6-color Gallios cytometer (Beckman Coulter, Brea, CA, USA) under a live gate of $CD11b/c^+$. Flow cytometric data were analyzed with the Kaluza flow analysis 1.3 software (Beckman Coulter). Microglia were defined as $CD11b/c^+$ $Granulocyte^-$ total, $MHCII^+$ and $CD172a^+$ subtypes. However, some macrophages might be included in the $CD11b/c^+$ $Granulocyte^-$ cells. Cell populations were calculated and presented as numbers of cells per mg tissue-weight, percentages among total microglia, or $MHCII^+/CD172a^+$ microglial ratios.

Microglia RNA isolation (CD11b positive cells)

Rats were perfused transcardially with 200 ml of 0.9% saline solution and a L1–L6 segment of the SC was collected for the isolation of CD11b immunopositive microglia/macrophages by magnetic-activated cell sorting (MACS). The tissue was dissociated using Neural tissue dissociation kit (T) (Miltenyi Biotec, San Diego, CA, USA; cat# 130-093-231) and the gentleMACS Dissociator (Miltenyi Biotec). After dissociation, the cells were suspended in 0.5% bovine serum albumin (BSA) in PBS and incubated with Myelin Removal Beads II (Miltenyi Biotec; cat# 130-096-733; 1:10 dilution) for 15 min at 4 °C. The cells were washed once and resuspended in 0.5% BSA in PBS and filtered through an LS column (Miltenyi Biotec; cat# 130-042-401) using a QuadroMACS Separator (Miltenyi Biotec). The total effluent was collected and resuspended in 0.5% BSA with 2 mM EDTA in PBS (washing buffer). The cells were incubated with mouse anti-CD11b:FITC antibody (AbD Serotec, Puchheim, Germany; Cat# MCA275FB; 1:10 dilution) at 4 °C for 10 min. The cells were washed once, resuspended in the washing buffer and incubated with anti-FITC MicroBeads (Miltenyi Biotec; cat# 130-048-701; 1:10 dilution) for 15 min at 4 °C. The cells were washed once and resuspended in the washing buffer. The cell suspension was applied to an LS column placed on a QuadroMACS Separator and the anti-CD11b-labeled cells were collected from the column for further experiments. RNA was extracted with Trizol reagent, alcohol-precipitated in the presence of glycogen and treated with DNase (#1906, Ambion).

In order to validate the purity of the isolate, we looked for known microglial markers, Cx3cr1, P2ry12, Ctss, Csf1r, and Cst3 (Denk et al., 2016; Butovsky et al., 2014). All the markers were expressed in the top

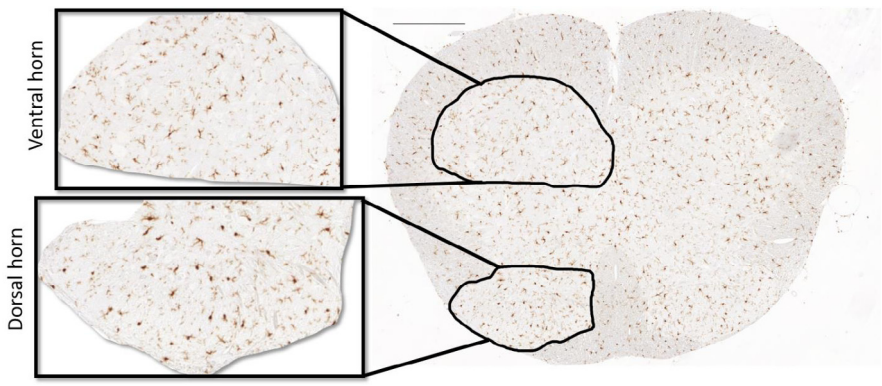

Fig. 1. Depiction of the definition of the dorsal and ventral horn of the spinal cord used in immunohistochemistry. The scale bar = 500 μm.

1% most of the expressed genes of the saline group in our data (data not shown).

RNA sequencing

Altogether 30 ng of total RNA was first submitted to rRNA and mitochondrial rRNA removal, using RiboGone – Mammalian–kit (Clonetech, Mountain View, CA, USA), and then used as a starting material for RNA-Seq. SMARTer® Stranded RNA-Seq Kit (Clonetech, Mountain View, CA, USA) was used to generate indexed cDNA libraries from 200 pg of the ribosomal/mitochondrial RNA-depleted RNA. Strand-specific sequencing data from the synthesized cDNA was obtained from the Illumina next generation sequencing system: the NextSeq High SE 1 × 75 bp run was used.

Initial quality control on sequenced reads was performed with FastQC v0.11.3. Based on the quality reports produced, Illumina adapters were removed by Trimmomatic v0.33 and the read files were preprocessed with the following settings: Reads with the first five bases were trimmed from the start of the read. Base quality scores less than 30 were trimmed from the 5′ end. Reads of length less than 20 bases were discarded. Had the samples had less than 70% of reads surviving trimming, they would have been discarded from further analysis.

The processed reads were then mapped to the reference genome (Rat Ensembl5) with Tophat v2.1.0 allowing for up to two mismatches (both in the initial read and the segmented read alignment) and enforcing rules for first-strand synthesis library type. The mapped reads were then quantified in fragments per kilobase of mapped reads (FPKM) with Cufflinks v2.2.1 using multiple read correction and upper-quartile normalization. Differential expression analysis was performed at the gene level using CuffDiff v2.2.1 with multiple read corrections.

The data (significantly impacted pathways and biological processes) were further analyzed using Advaita Bio's iPathwayGuide (http://www.advaitabio.com/ipathwayguide).

Statistical analysis

In the text and figures, results are presented as mean of the sample values + standard error of the mean (SEM). The behavioral data were tested for statistically significant differences in the mean values by two-way analysis of variance repeated-measures followed by a two-tailed Holm–Sidak correction for multiple comparisons. For the cold-plate test results the data from day 14 were analyzed using unpaired two-tailed *T*-test with Welch's correction. The immunohistochemistry data (Iba1 and GFAP staining) were tested for statistically significant differences by two-way analysis of variance followed by a two-tailed Holm–Sidak correction for multiple comparisons, except for the CGRP and substance P staining that were analyzed with unpaired two-tailed *T*-test with Welch's correction. Fluorescence-activated cell sorting (FACS) data were tested for statistically significant differences with unpaired two-tailed *T*-test with Welch's correction. Differentially expressed (DE) genes were defined to have a *q*-value (False Discovery Rate adjusted *p*-value) < 0.05. In the iPathway analysis, the differential expression threshold for the gene fold change was set to 0.5 (log 2) and *q*-value 0.05. False discovery rate *p*-value correction was applied for GO-enrichment analysis and impacted phenotype analysis. The difference was considered significant at $p < 0.05$.

RESULTS

Antinociceptive tolerance and hyperalgesia following repeated morphine administration

Behavioral signs of morphine antinociceptive tolerance and hyperalgesia were seen in the rats during the experimental period of 13 days. On day 1, morphine 10 mg/kg s.c. caused a cut-off latency of 10 s in the tail flick test 1 h after administration, whereas the mean latency in the saline-treated rats was 3.2 s ($p < 0.01$, Fig. 2A). In similar measurements on days 3 and 7, the mean tail flick latencies after morphine 10 mg/kg gradually decreased to 8.2 and 6.7 s, respectively (Fig. 2A). Complete tolerance to the antinociceptive effect of morphine had developed by day 10 (Fig. 2A). Chronic morphine treatment failed to significantly change the baseline values in the tail flick test on days 3, 7, 10, and 13 (12 h from the last morphine injection) compared with the saline group (Fig. 2A).

The Dynamic Plantar Aesthesiometer test (DPA) was measured on days 1, 3, 7, 10, and 13 (12 h from the last morphine injection on days 3, 7, 10, and 13). The threshold observed for morphine-treated rats was decreased compared with saline-treated rats on day 10 ($p < 0.05$, Fig. 2B). On days 1, 3, 7, and 13, there were no significant differences between the groups (Fig. 2B).

The cold plate test was performed on days 8, 12, and 14 (12 h from the last morphine injection). The nociceptive latency of the morphine-treated rats was significantly decreased compared with the saline group on days 8 and 12 (Fig. 2C). Despite the trend, the difference between the treatment and control groups failed to reach significance on day 14 (Fig. 2C).

Morphine increases immunoreactivity of microglial marker Iba1, substance P, and CGRP in SC

To determine whether chronic morphine treatment leads to an increase in the number or area of glial cells in the SC and brain, we analyzed the cells expressing Iba1 and GFAP, commonly used markers of microglia and astrocytes, respectively.

SC IBA1: Representative samples of dorsal and ventral horn Iba1 staining of both treatment groups are shown in Fig. 3A. Compared with saline-treated animals, the number of cells was increased in the dorsal horn in the morphine group by 33% ($p < 0.01$, Fig. 3B). The area of positive staining per area of tissue was increased in the dorsal horn in the morphine group compared with the saline group by 32% ($p < 0.01$,

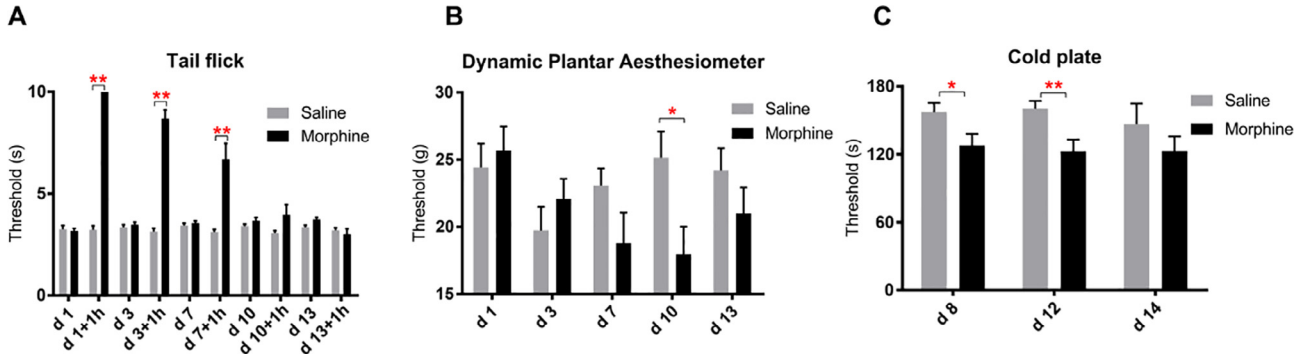

Fig. 2. Antinociceptive tolerance and hyperalgesia following repeated morphine administration. The effect of morphine in the tail flick (A), dynamic plantar aesthesiometer (B), and cold plate (C) tests. The rats were administered morphine 10 mg/kg, s.c. or saline twice daily for 14 days. The baseline values (12 h after the last morphine injection, except on day 1) were measured with all nociceptive tests. The tail flick test was also performed one hour after the morphine injection on every measurement day. Statistically significant difference $^{*}p < 0.05$, $^{**}p < 0.01$ as compared with saline control. $n = 14–15$ rats per group, except for the cold plate test on day 14, where $n = 10–11$ rats per group.

Fig. 3C) and in the ventral horn by 23% ($p < 0.05$, Fig. 3C).

SC GFAP: Representative samples of dorsal and ventral horn GFAP stainings of saline and morphine treatment groups are shown in Fig. 4A. Compared with the saline group, chronic morphine administration failed to change the number of cells expressing GFAP (Fig. 4B) or the area of positive staining per area (Fig. 4C) in the dorsal or ventral horns.

To determine whether chronic morphine treatment leads to an increase in the neuropeptides that are reported to activate glia, we analyzed the area covered by CGRP and substance P positive immunoreactivity in dorsal horn of the SC.

SC CGRP and substance P. The area covered by substance P-positive staining was increased in the dorsal horn in the morphine group compared with the saline group by 109% ($p < 0.05$, Fig. 5A) and CGRP-positive staining by 106% ($p < 0.01$, Fig. 5B). Representative photomicrographs of substance P- and CGRP-positive stainings are shown in Fig. 5C, D.

Morphine fails to increase Iba1 and GFAP immunoreactivity in the brain areas relevant for pain processing

Brain IBA1. Compared with the saline group, the number of cells was decreased in the substantia nigra in the morphine group by 39% ($p < 0.05$, Fig. 6A). In the striatum, forelimb area of cortex, nucleus accumbens, ventral posterolateral nucleus, medial dorsal nucleus, central amygdala, ventral tegmental area, central gray, and rostroventral medulla, the number of cells were not significantly changed (Fig. 6A). The areas of positive staining per areas of tissue were not significantly changed between the morphine and saline groups in any of the studied brain areas (Fig. 6C).

Brain GFAP. The number of cells or the area of positive staining per area of tissue was statistically unchanged in the studied brain regions (Fig. 6B, D).

In flow cytometry, the total amount of microglia decreases in the medulla and the proportion of M2-polarized microglia increases in the SC after morphine treatment

Next we used flow cytometry to complement the immunohistochemistry analysis. In flow cytometry, the total amount of microglia was decreased by 13% ($p < 0.05$) in the morphine-treated group compared with the saline group in the medulla (Fig. 7A). In the sensory cortex and SC, the amount of microglia was not significantly changed between the morphine and saline groups (Fig. 7B, C). Compared with the saline group, morphine treatment increased the proportion (%) of M2-(CD172a+) microglia in total microglia in the SC by 70% ($p < 0.01$, Fig. 7C), but not in the medulla and sensory cortex. The proportion of M1-microglia of the total microglia was not otherwise significantly changed between the morphine and saline groups in the medulla, sensory cortex, or SC. Examples and gating strategy for total microglia, M1-, and M2-microglia in saline and morphine treatment are shown in the SC in Fig. 7D.

Repeated morphine administration changes RNA transcriptomics in spinal microglia – expression of the DAP12 pathway genes is significantly upregulated

The transcriptomics was performed on microglia cells (CD11b+) isolated from the SCs of three rats from both morphine and saline-treatment groups to assess the morphine-induced transcriptional changes in microglia. The differential expression (DE) analysis detected 2454 differentially expressed genes between the treatment groups.

In the gene ontology (GO) enrichment analysis, the following GO terms were significantly enriched: immune system process, responses to stress, catabolic process, defense response, organic substance catabolic process, cell activation, and cellular catabolic process. In the impacted phenotype pathway analysis, the genes related to the phagosome route were significantly over-represented. Expression of the genes of the DAP12 pathway (Kobayashi et al., 2016), *Trem2, Tyrobp, Irf8,*

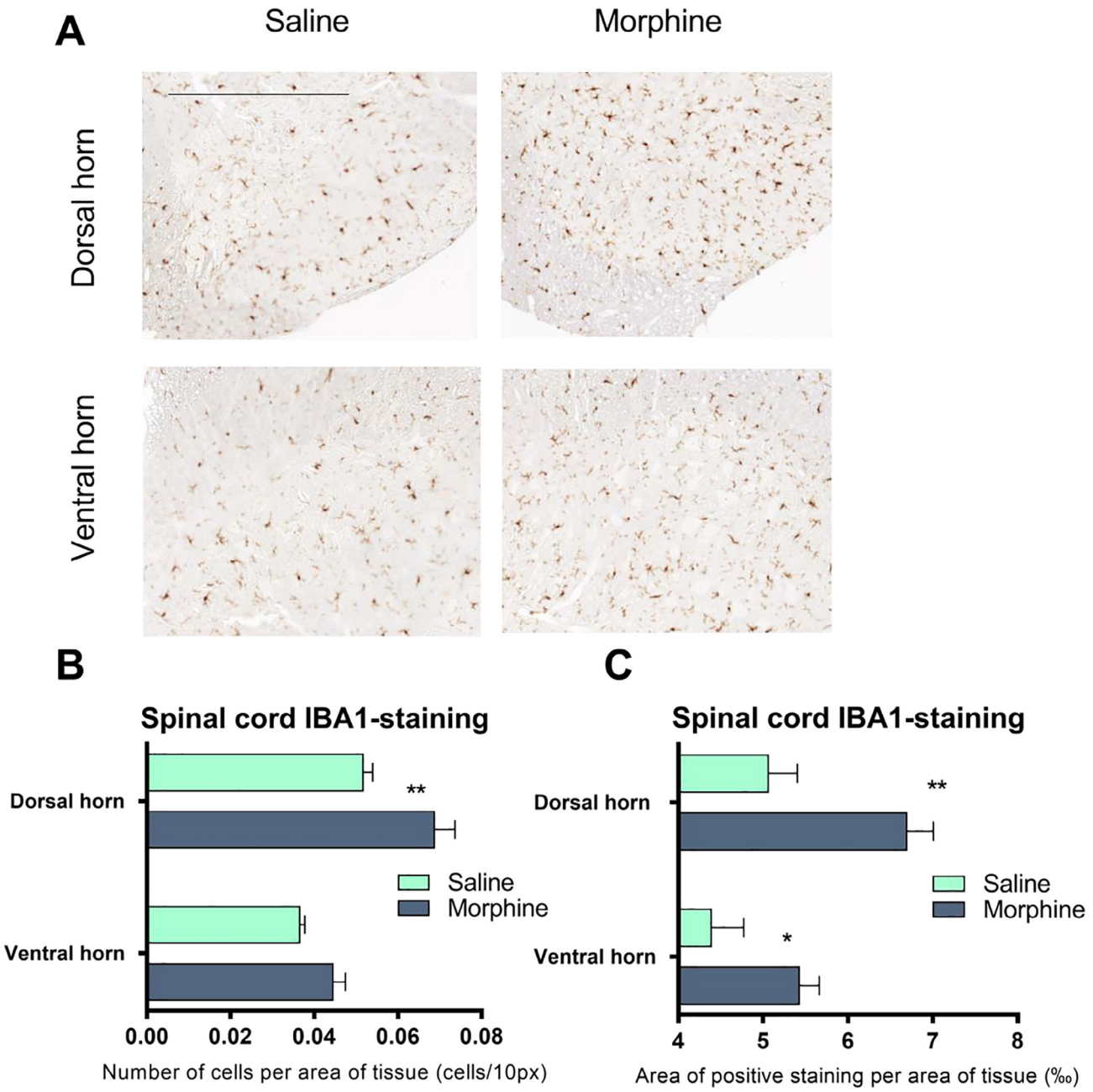

Fig. 3. Morphine increases Iba1 immunoreactivity in spinal cord. Representative photomicrographs of the saline and morphine treatment groups of dorsal and ventral horn are shown in the top row (A). The number of cells per area of tissue (B) and area of positive staining per area of tissue (C) in the dorsal and ventral horn of the spinal cord with Iba1 staining after morphine 10 mg/kg, s.c. or saline twice a day for 14 days. Statistically significant difference $^{*}p < 0.05$, $^{**}p < 0.01$ as compared with the saline control. $n = 5$ in both groups. The scale bar = 500 μm.

Irf5, and *P2xr4* were significantly upregulated (Table 1). Other DAP12 pathway related genes (*Cx3cr1*, *Ctss*, and *Csf1r*) were also upregulated, but the change was statistically non-significant (Table 1). In addition, other individual genes were significantly upregulated, including: *Kcnn4*, *Fkbp5, Fcgr1a, and Cd244* (Table 1).

DISCUSSION

We found that chronic morphine treatment induced tolerance and hyperalgesia in the rat. The treatment also increased the number of microglial cells in the dorsal and ventral horns of the SC and immunoreactivity of substance P and CGRP in the dorsal horn. However, neither the number nor the area of astrocytes in the SC was changed. In flow cytometry, morphine treatment increased the proportion of M2-polarized microglia in the SC but did not change either the number or the proportion of M1-polarized microglia. In the transcriptome of the microglial cells isolated from the SC, morphine treatment increased the transcripts related to cell activation and defense response. Interestingly, in this study, glial reactivity increased only at the spinal but not supraspinal level. In the studied

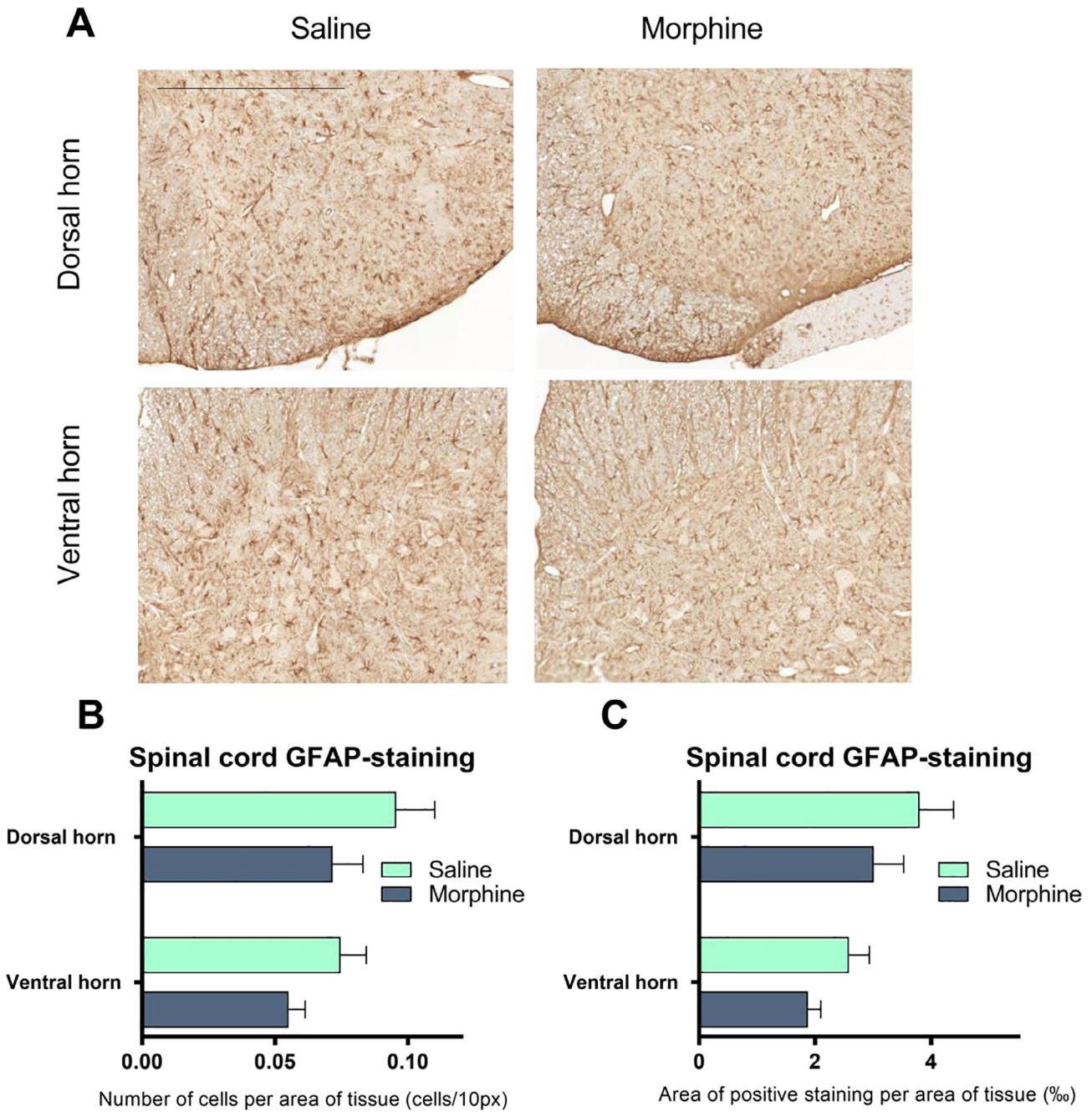

Fig. 4. Morphine does not increase GFAP immunoreactivity in spinal cord. Representative photomicrographs of dorsal and ventral horn GFAP stainings of both treatment groups (A). The Number of cells per area of tissue (B) or area of positive staining per area of tissue (C) in the dorsal and ventral horn of spinal cord with GFAP staining after morphine 10 mg/kg, s.c. or saline injections twice daily for 14 days. $n = 5$ in both groups. The scale bar = 500 μm.

brain regions, immunohistochemistry showed no changes in the number or area of microglia or astrocytes, except for a decrease in the number of microglial cells in the substantia nigra. In flow cytometry, morphine treatment reduced the number of microglial cells in the medulla with no change in the proportion of M1- and M2-polarized microglia.

In this study, the rats became tolerant to the antinociceptive effect of morphine after a ten-day morphine treatment. Signs of opioid-induced hyperalgesia were detected in both mechanical and cold nociceptive tests 12 h after morphine injection. Concurrently, the treatment increased the number of microglial cells by 33% in the dorsal horn of the SC when the classical microglia marker Iba1 was used. In the ventral horn, the area of microglial cells increased by 24%, which we consider to be related to the increase in the cell number, as the number of cells was increased 22%, although not significantly.

The increase of microglial cells in the dorsal horn is in agreement with previous studies that have described the activation of glia after chronic morphine treatment

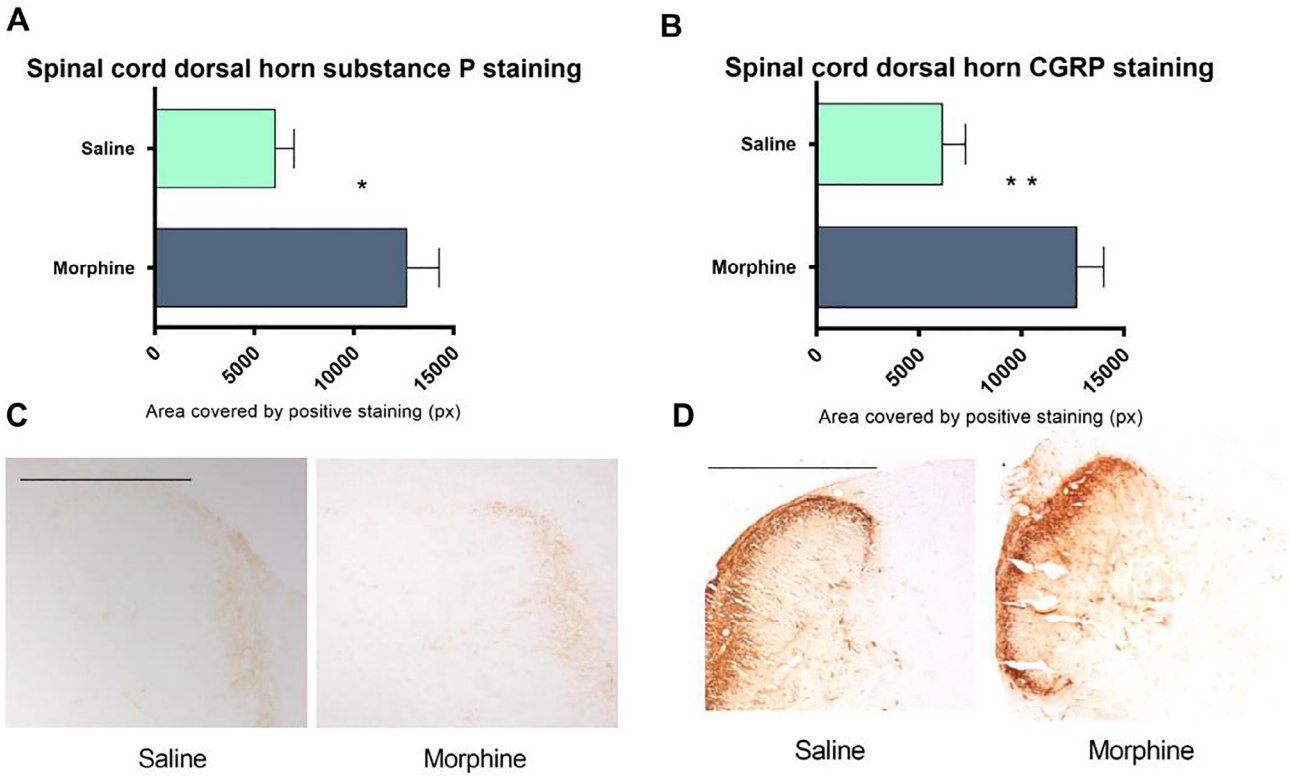

Fig. 5. Morphine enhances substance P and calcitonin gene-related peptide immunoreactivity in spinal cord. Area covered by substance P (A) and CGRP (B) -positive staining in the dorsal horn of the spinal cord after morphine 10 mg/kg, s.c. or saline twice daily for 14 days. Representative photomicrogprahs of substance P (C) and CGRP (D) -positive staining in both treatment groups. Statistically significant $^{*}p < 0.05$, $^{**}p < 0.01$ as compared with the saline control. $n = 4–5$ in both groups. The scale bar = 500 μm.

(Raghavendra et al., 2002; Holdridge et al., 2007; Cui et al., 2008; Mattioli et al., 2010; Wang et al., 2010). The magnitude of the change in microglial immunoreactivity is also in the same range as previously reported by Holdridge et al. (60%) after systemic administration of morphine. Larger increases have been detected (300%) after subarachnoid administration of morphine (Cui et al., 2008).

Both proliferation and hypertrophy of microglia have been described as a response to insult (Gwak et al., 2012) and they both are considered to reflect activation of glia (Ji et al., 2013). In agreement with the studies of Jun et al (Jun et al., 2013) and Wang et al (Wang et al., 2010) our results suggest that the opioid-induced spinal microglia activation might not be restricted to hypertrophy and could resemble that of the peripheral nerve injury where microglia proliferation (Melzer et al., 1997; Echeverry et al., 2008) has been detected.

Interestingly, systemic administration of high doses of morphine also increased the number of microglial cells in the ventral horn. Cui et al. have also shown that subarachnoid administration of chronic morphine causes activation of microglia but not astrocytes in the ventral horn (Cui et al., 2006). There is some evidence to suggest that opioid-induced neuroinflammation in the ventral horn could have pathological consequences. High doses of subarachnoid morphine (40 μg × 2 daily) have been reported to induce paraplegia with degeneration of spinal ventral neurons (Kakinohana et al., 2007).

Our understanding of how morphine activates glia remains incomplete. Recent reports suggest that no μ-opioid receptors are expressed in the microglia or astrocytes in the SC of naïve or morphine-treated animals (Kao et al., 2012; Corder et al., 2017). Toll-Like Receptor 4 (TLR-4) has been suggested to be a key mediator in opioid-induced activation or microglia (Watkins et al., 2009). Its role in morphine-induced tolerance and hyperalgesia, however, has also been questioned, as neither were altered in TLR4 null mice (Mattioli et al., 2014). In our study, chronic morphine treatment increased the neuron-derived peptides substance P and CGRP in the dorsal horn, which agrees with previous reports (Powell et al., 2000; Melik Parsadaniantz et al., 2015). Both substance P (Zhu et al., 2014) and CGRP (Reddington et al., 1995) have been shown to activate glial cells. Thus, it is possible that morphine effects on glial cells are μ-opioid-receptor independent.

A diverse set of activated microglial phenotypes has been identified (Luo and Chen, 2012). Thus, the classical approach that utilizes single histochemical markers might provide an incomplete picture of the activation as microglial cells, which have different properties with some of them having pro- and others anti-inflammatory effects. Therefore, we wanted to investigate the activated microglia in more detail using flow cytometry. The M1 (pro-inflammatory) and M2 (anti-inflammatory)-paradigm has been used to polarize microglial phenotypes according to

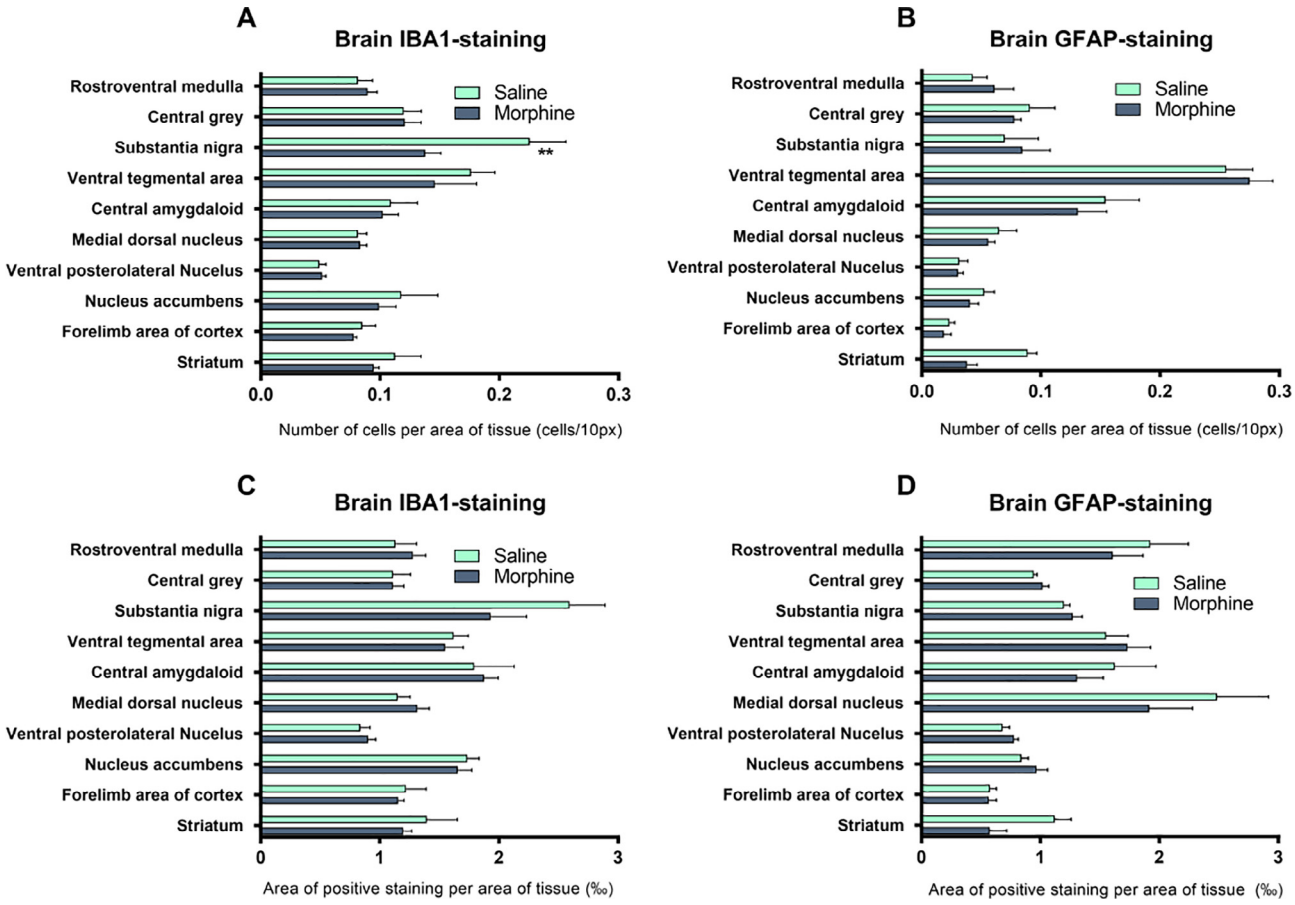

Fig. 6. Morphine does not increase Iba1-associated microglia or GFAP immunoreactivity in the brain. Number of cells per area of tissue (A, B) or area of positive staining per area of tissue (C, D) in the referred brain regions with IBA1 and GFAP-staining after morphine 10 mg/kg, s.c. or saline twice a day for 14 days. Statistically significant difference $^{**}p < 0.01$ as compared with the saline group. $n = 5$ in both groups.

their functional properties regarding inflammation (Franco and Fernandez-Suarez, 2015; Tang and Le, 2016). M1/2 microglia activation was not studied previously in the context of chronic morphine administration. We defined M2 microglia according to high expression of CD172a (SIRPα), which has been shown to prevent phagocytosis and to exert anti-inflammatory properties when paired with CD47 (Latour et al., 2001; Barclay and Van den Berg, 2014; Gitik et al., 2014). It should be stated, however, that the concept of M1 and M2 polarization may over-simplify the broad spectrum of microglial activation phenotypes, but also that heterogeneity of microglial populations is not only limited to M1/2 phenotypes (Cherry et al., 2014; Chen and Trapp, 2016; Ransohoff, 2016). The activation of microglia seems to be context-dependent (Cherry et al., 2014). This would be in harmony with the idea that microglia need to be able to react to a diverse set of external challenges. Thus, a limitation of this study was that we used only one marker per cell type, MHCII+ to define M1-microglia and CD172a+ to define M2-microglia, which account for only a fraction of the total microglia. Furthermore, it should be mentioned that CD11b/c+ which was used to define microglia is also associated with macrophages.

In our investigation, the increased proportion of M2-microglia in the SC could be interpreted as an effort to resolve the neuroinflammation caused by chronic morphine administration. Analogously, a rise in the proportion of similarly defined M2-microglia in the SC has been detected seven days after peripheral nerve injury in the rat (Li et al., 2016). In accordance with this hypothesis, parthenolide, known to affect intracellular microglial inflammation pathways, like p-38 and ERK1/2 (Popiolek-Barczyk et al., 2015), has promoted spinal M2 microglia/-macrophage polarization and relieved pain in a rat model of neuropathy (Popiolek-Barczyk et al., 2015). Considering the role of activated glia in both neuropathic pain and opioid-induced neuroinflammation, drugs that promote M2-conversion of spinal microglia could be beneficial also in the treatment of OIH and attenuation of morphine tolerance.

In flow cytometry, the total amount of microglia ($CD11b/c^{+}$ $Granulocyte^{-}$) and the proportion of the pro-inflammatory M1-microglia ($CD172^{-}MHCII^{+}$) were unchanged in the SC after morphine treatment. Flow cytometry differentiates the cells by the expression levels of the used antibodies and the microglia populations defined this way may not necessarily correspond with those characterized by immunohistochemistry. Thus, assays using both immunohistochemistry and flow cytometry might provide a complementary way to assess microglial activation.

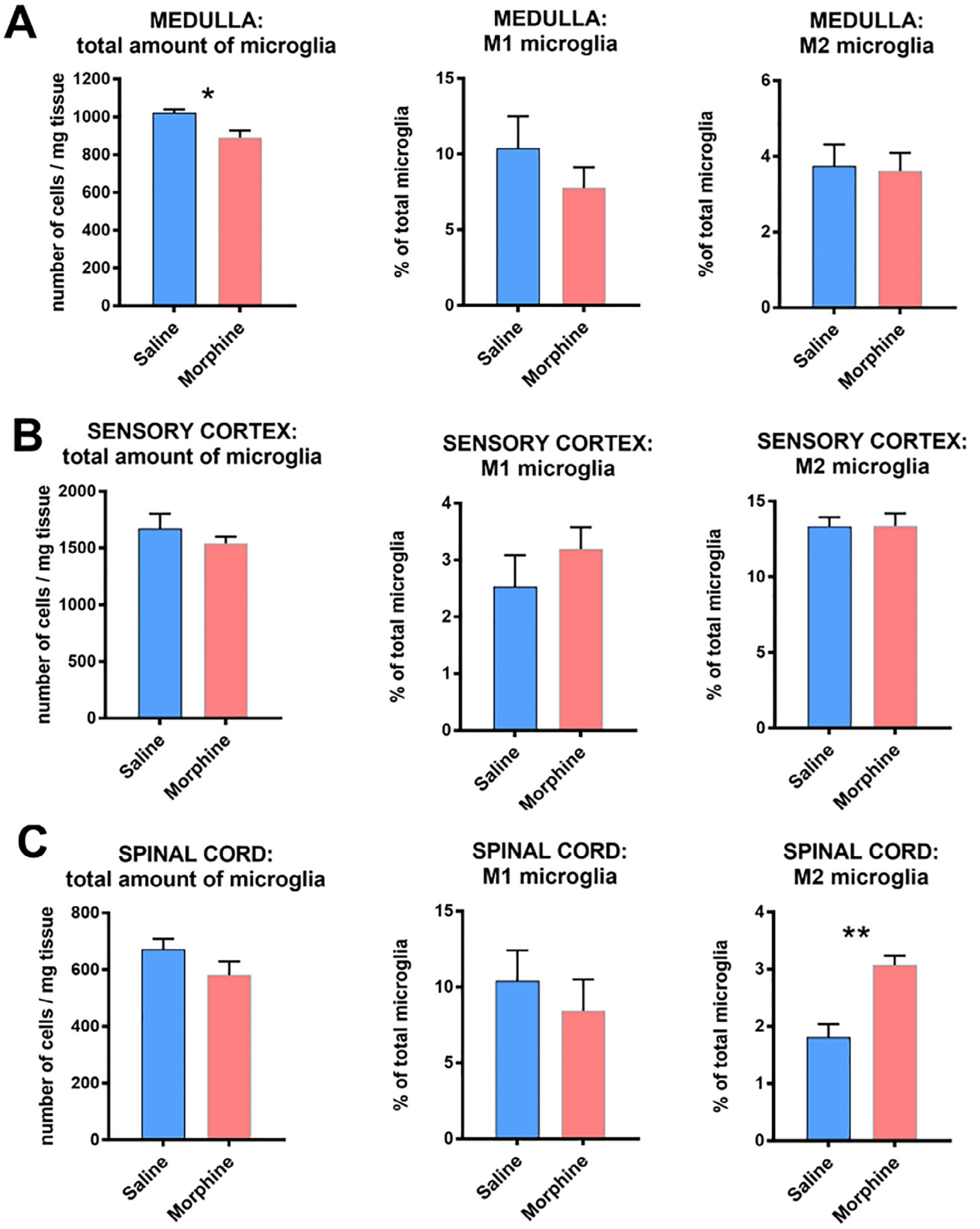

Fig. 7. In flow cytometry, the total amount of microglia decreases in the medulla and the proportion of M2-polarized microglia increases in the spinal cord after morphine treatment. The number of microglial cells per mg tissue and the proportion of M1 and M2 microglia among total microglia in medulla (A), sensory cortex (B), and spinal cord (C) after morphine 10 mg/kg, s.c. or saline twice a day for 14 days. Statistically significant difference $^{*}p < 0.05$, $^{**}p < 0.01$ as compared to the saline group. $n = 4–5$ in both groups. Example of gating strategies of saline- and morphine-treated samples of the total microglia ($CD11b/c^{+}$), M1 ($MHCII^{+}$), and M2 ($CD172a^{+}$) microglia for the spinal cord (D). MG/Mϕ = Microglia/macrophage.

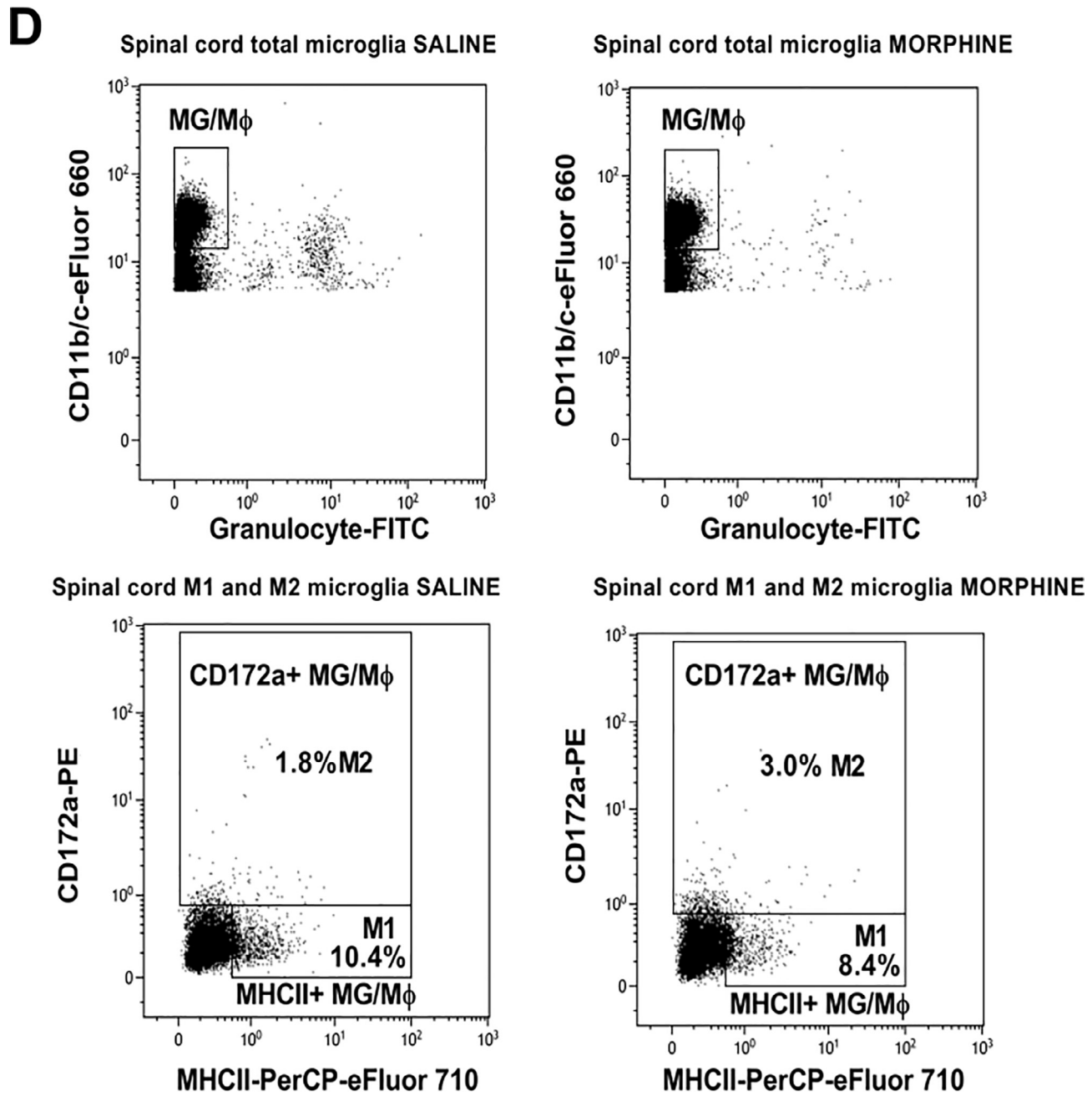

Fig. 7 (*continued*)

To gain more insight to the intracellular effects of chronic morphine, transcriptome analysis of the isolated spinal microglia was performed. In the analysis, the following GO terms were significantly enriched: immune system process, response to stress catabolic process, defense response, organic substance catabolic process, cell activation, and cellular catabolic process. In addition, the genes in the 'phagosome' phenotype pathway were over-represented. Interestingly, the phagosome pathway has also been shown previously to be activated after the administration of bacterial lipopolysaccharide in mouse microglia and to associate to the loss of dopaminergic neurons (Bodea et al., 2014). The results would indicate that morphine acts as a noxious stimulus to microglia.

Many renowned individual genes related to pain and inflammatory activation were also differentially expressed. We found that the DAP12 pathway associated genes (Guan et al., 2016), *Tyrobp, Irf8, Irf5*, and *P2rx4*, were significantly up-regulated. *Csf1r*, *Cx3cr1*, and *Ctss* were also up-regulated, but the change was non-significant. The DAP12 pathway, along with its individual downstream molecules, has been suggested to be an essential contributor to neuropathic pain

Table 1. Changes of expression levels of individual genes in microglia. Microglial cells were isolated from the spinal cord after chronic morphine treatment 10 mg/kg, s.c. or saline twice daily for 14 days. The results are quantified in log2-fold change of morphine *vs* saline-treatment groups. $n = 3$ in both groups. [1]Fragments Per Kilobase of exon per Million fragments mapped. [2]False Discovery Rate adjusted *p*-value

	Gene name	Fold Change Morphine/Saline (FPKM[1] log2)	q-value[2]
	Kcnn4	3.54	0.003
	Fkbp5	3.14	0.001
	Fcgr1a	0.76	0.002
	Cd244	1.06	0.001
DAP12 pathway	*Trem2*	1.11	0.001
DAP12 pathway	*Tyrobp*	0.90	0.001
	Cx3cr1	0.52	0.124
DAP12 pathway	*Ctss*	0.49	0.390
DAP12 pathway	*Irf8*	0.64	0.015
DAP12 pathway	*Irf5*	0.86	0.001
DAP12 pathway	*P2rx4*	0.66	0.030
DAP12 pathway	*Csf1r*	0.68	0.125

(Guan et al., 2016; Kobayashi et al., 2016). Our data also included other DE genes that have been highlighted in neuropathic pain such as *Cd244*, *Fcgr1* (Denk et al., 2016). Interestingly, we also detected upregulation of *Fkbp5*. Silencing of *Fkbp51* (same as *Fkbp5*) in the SC has led to reduced hypersensitivity in a rodent model of neuropathic pain (Maiaru et al., 2016) but no study has yet demonstrated its up-regulation in microglia in association with chronic morphine treatment. *Kcnn4* has been shown to promote microglial activation and consequent neurotoxicity (Kaushal et al., 2007), and it is up-regulated in M2-microglia where it promotes cell migration (Ferreira et al., 2014). Activation of TREM2 elicits a pro-inflammatory response in microglia and exacerbates neuropathic pain in the DAP12/TREM2 pathway (Kobayashi et al., 2016).

Opioid-induced activation of glia has been less studied in the supraspinal structures than in the SC. Although the role of the SC in the transmission and modulation of nociception is crucial, it constitutes only part of the structures critical for the processing of nociception and pain. For example, in humans, nucleus accumbens has been shown to be involved in the transition to chronic pain (Baliki et al., 2010) and the amygdala contributes to the negative affective states related to pain (Veinante et al., 2013).

In our study, neither the count nor the area of microglia or astrocytes were significantly changed in the striatum, forelimb area of cortex, nucleus accumbens, ventral posterolateral nucleus, medial dorsal nucleus, central amygdala, ventral tegmental area, central grey, or rostroventral medulla. Previous literature regarding the activation of supraspinal glia after chronic morphine is inconsistent. For example, the immunoreactivity of microglia was increased in nucleus accumbens in the study of Zhang et al. (2012) but decreased in a study by Hutchinson et al. (2009). Activation of microglia in the periaqueductal grey was detected by Hutchinson et al. (2009) and Eidson and Murphy (2013), but not by Bajic et al. (2013). Nonetheless, supraspinal activation of astrocytes and microglia has been detected in the ventral tegmental area after opioid administration (Hutchinson et al., 2009; García-Pérez et al., 2016; Taylor et al., 2016). The discrepancy with our results and others could be related to the differences in the study settings, like the morphine tolerance induction scheme and the rat strain. In our study we looked at both spinal and supraspinal glial activation and showed activation in the spinal but not in the supraspinal level. Thus it could be hypothesized that glial activation in the studied supraspinal structures might not be necessary for the development of tolerance or opioid-induced hyperalgesia. This is in agreement with a recent study suggesting that supraspinal structures are not required for the development of opioid tolerance and OIH (Corder et al., 2017).

Some of the findings of this study were surprising, including the reduced microgliosis in the substantia nigra and medulla and the increased immunoreactivity of microglia in the ventral horn. Because the ventral horn of the SC is part of the pyramidal pathway,

important in voluntary movements, and the substantia nigra modulates movement through the extrapyramidal system, it would be tempting to hypothesize that the effects of chronic morphine on activation of microglia would affect motor function. Chronic use of high doses of opioids is known to occasionally associate with myoclonus in humans (Bowdle and Rooke, 1994; Mercadante, 1998). However, the possible effects of reduced microgliosis in the substantia nigra to the processing of nociception and pain cannot be excluded. Intranigral microinjection of naloxone has suppressed the antinociceptive effects of systemically administered morphine in thermal nociceptive tests in a dose-related manner (Baumeister et al., 1988). Hypersensitivity to noxious stimulation has also been reported to possibly be involved in unilateral dopamine depletion in the nigrostriatal pathway in the rat (Maegawa et al., 2015).

Morphine-induced glia-mediated neuroinflammation is a complex molecular system and it is probable that multiple subpopulations of glia are involved in its initiation and resolution. Identifying the relevant pathological glial populations as well as the vulnerable neuroanatomical systems, such as the substantia nigra, is important in order to understand the possible neurodegenerative consequences of long-term opioid administration. It cannot be excluded that Iba1 and GFAP immunostainings were unable to demonstrate the relevant populations of glia and in that case other approaches should be used to study this in more depth. The use of advanced methods like flow cytometry and RNA sequencing can provide detailed information of the glial activation and help to determine more useful biomarkers, as well as to develop new treatment methods.

CONCLUSION

We presented a comprehensive set of data on glial activation in the SC and brain. Our results suggest that microglial activation associated with opioid tolerance and opioid-induced hyperalgesia occurs mainly at the spinal level. The transcriptome data suggest that the pattern of microglial activation after chronic morphine treatment is similar to that of neuropathic pain.

DISCLOSURE STATEMENT

Pekka Rauhala works as a part-time medical advisor in Orion Pharma, otherwise the authors have nothing to disclose.

ACKNOWLEDGMENTS

Biomedicum Functional Genomics Unit (FuGU) and Dr. Catherine Icay are acknowledged for their technical work and providing the original method protocols. Institute of Biotechnology, University of Helsinki is acknowledged (http://www.biocenter.helsinki.fi/bi/histoscanner/index.html). The research leading to these results has received funding from the European Union Seventh Framework Programme (FP7/2007–2013) under grant agreement no 602919, Finnish Medical Society (Finska Läkaresällskapet), University of Helsinki 375th Anniversary Grant, University of Helsinki, and Centre for International Mobility of Finland CIMO.
VJ designed the study, performed experiments, analyzed data, and wrote the first draft of the MS. TL, YS, HV, and PR designed the study, performed experiments, analyzed data, and participated in the writing of the MS. IS, MA, KM, JA, ZL, and HT performed experiments, analyzed data, and participated in the writing of the MS. EK and LT designed the study, analyzed data, and participated in the writing of the MS.

REFERENCES

Allchorne AJ, Broom DC, Woolf CJ (2005) Detection of cold pain, cold allodynia and cold hyperalgesia in freely behaving rats. Mol Pain 1:36.

Bajic D, Commons KG, Soriano SG (2013) Morphine-enhanced apoptosis in selective brain regions of neonatal rats. Int J Dev Neurosci 31:258–266.

Baliki MN, Geha PY, Fields HL, Apkarian AV (2010) Predicting value of pain and analgesia: nucleus accumbens response to noxious stimuli changes in the presence of chronic pain. Neuron 66:149–160.

Barclay AN, Van den Berg TK (2014) The interaction between signal regulatory protein alpha (SIRPalpha) and CD47: structure, function, and therapeutic target. Annu Rev Immunol 32:25–50.

Baumeister AA, Anticich TG, Hawkins MF, Liter JC, Thibodeaux HF, Guillory EC (1988) Evidence that the substantia nigra is a component of the endogenous pain suppression system in the rat. Brain Res 447:116–121.

Bodea L-G, Wang Y, Linnartz-Gerlach B, Kopatz J, Sinkkonen L, Musgrove R, Kaoma T, Muller A, Vallar L, Di Monte DA, Balling R, Neumann H (2014) Neurodegeneration by activation of the microglial complement-phagosome pathway. J Neurosci 34:8546–8556.

Bowdle TA, Rooke GA (1994) Postoperative myoclonus and rigidity after anesthesia with opioids. Anesth Analg 78:783–786.

Butovsky O, Jedrychowski MP, Moore CS, Cialic R, Lanser AJ, Gabriely G, Koeglsperger T, Dake B, Wu PM, Doykan CE, Fanek Z, Liu L, Chen Z, Rothstein JD, Ransohoff RM, Gygi SP, Antel JP, Weiner HL (2014) Identification of a unique TGF-beta-dependent molecular and functional signature in microglia. Nat Neurosci 17:131–143.

Caraceni A, Hanks G, Kaasa S, Bennett MI, Brunelli C, Cherny N, Dale O, De Conno F, Fallon M, Hanna M, Haugen DF, Juhl G, King S, Klepstad P, Laugsand EA, Maltoni M, Mercadante S, Nabal M, Pigni A, Radbruch L, Reid C, Sjogren P, Stone PC, Tassinari D, Zeppetella G, European Palliative Care Research Collaborative (EPCRC)European Association for Palliative Care (EAPC) (2012) Use of opioid analgesics in the treatment of cancer pain: evidence-based recommendations from the EAPC. Lancet Oncol 13:58–68.

Chen Z, Trapp BD (2016) Microglia and neuroprotection. J Neurochem 136(Suppl. 1):10–17.

Cherry JD, Olschowka JA, O'Banion MK (2014) Neuroinflammation and M2 microglia: the good, the bad, and the inflamed. J Neuroinflammation 11:98.

Corder G, Tawfik VL, Wang D, Sypek EI, Low SA, Dickinson JR, Sotoudeh C, Clark JD, Barres BA, Bohlen CJ, Scherrer G (2017) Loss of mu opioid receptor signaling in nociceptors, but not microglia, abrogates morphine tolerance without disrupting analgesia. Nat Med 23:164–173.

Cova JL, Aldskogius H, Arvidsson J, Molander C (1988) Changes in microglial cell numbers in the spinal cord dorsal horn following brachial plexus transection in the adult rat. Exp Brain Res 73:61–68.

Cui Y, Chen Y, Zhi J-L, Guo R-X, Feng J-Q, Chen P-X (2006) Activation of p38 mitogen-activated protein kinase in spinal

microglia mediates morphine antinociceptive tolerance. Brain Res 1069:235–243.
Cui Y, Liao X-X, Liu W, Guo R-X, Wu Z-Z, Zhao C-M, Chen P-X, Feng J-Q (2008) A novel role of minocycline: attenuating morphine antinociceptive tolerance by inhibition of p38 MAPK in the activated spinal microglia. Brain Behav Immun 22:114–123.
Denk F, Crow M, Didangelos A, Lopes DM, McMahon SB (2016) Persistent Alterations in Microglial Enhancers in a Model of Chronic Pain. Cell Rep 15:1771–1781.
Echeverry S, Shi XQ, Zhang J (2008) Characterization of cell proliferation in rat spinal cord following peripheral nerve injury and the relationship with neuropathic pain. Pain 135:37–47.
Eidson LN, Murphy AZ (2013) Persistent peripheral inflammation attenuates morphine-induced periaqueductal gray glial cell activation and analgesic tolerance in the male rat. J Pain 14:393–404.
Ferreira R, Lively S, Schlichter LC (2014) IL-4 type 1 receptor signaling up-regulates KCNN4 expression, and increases the KCa3.1 current and its contribution to migration of alternative-activated microglia. Front Cell Neurosci 8:183.
Franco R, Fernandez-Suarez D (2015) Alternatively activated microglia and macrophages in the central nervous system. Prog Neurobiol 131:65–86.
García-Pérez D, Laorden ML, Milanés MV (2016) Regulation of pleiotrophin, midkine, receptor protein tyrosine phosphatase β/ζ, and their intracellular signaling cascades in the nucleus accumbens during opiate administration. Int J Neuropsychopharmacol:19.
Gitik M, Kleinhaus R, Hadas S, Reichert F, Rotshenker S (2014) Phagocytic receptors activate and immune inhibitory receptor SIRPα inhibits phagocytosis through paxillin and cofilin. Front Cell Neurosci:8.
Grace PM, Maier SF, Watkins LR (2015) Opioid-induced central immune signaling: implications for opioid analgesia. Headache 55:475–489.
Guan Z, Kuhn JA, Wang X, Colquitt B, Solorzano C, Vaman S, Guan AK, Evans-Reinsch Z, Braz J, Devor M, Abboud-Werner SL, Lanier LL, Lomvardas S, Basbaum AI (2016) Injured sensory neuron-derived CSF1 induces microglial proliferation and DAP12-dependent pain. Nat Neurosci 19:94–101.
Gwak YS, Kang J, Unabia GC, Hulsebosch CE (2012) Spatial and temporal activation of spinal glial cells: role of gliopathy in central neuropathic pain following spinal cord injury in rats. Exp Neurol 234:362–372.
Hains BC, Waxman SG (2006) Activated microglia contribute to the maintenance of chronic pain after spinal cord injury. J Neurosci 26:4308–4317.
Holdridge SV, Armstrong SA, Taylor AMW, Cahill CM (2007) Behavioural and morphological evidence for the involvement of glial cell activation in delta opioid receptor function: implications for the development of opioid tolerance. Mol Pain 3:7.
Hutchinson MR, Lewis SS, Coats BD, Skyba DA, Crysdale NY, Berkelhammer DL, Brzeski A, Northcutt A, Vietz CM, Judd CM, Maier SF, Watkins LR, Johnson KW (2009) Reduction of opioid withdrawal and potentiation of acute opioid analgesia by systemic AV411 (ibudilast). Brain Behav Immun 23:240–250.
Ji R-R, Berta T, Nedergaard M (2013) Glia and pain: is chronic pain a gliopathy? Pain 154(Suppl. 1):S10–S28.
Jun I-G, Kim S-H, Yoon Y-I, Park J-Y (2013) Intrathecal lamotrigine attenuates antinociceptive morphine tolerance and suppresses spinal glial cell activation in morphine-tolerant rats. J Kor Med Sci 28:300–307.
Kakinohana M, Oshiro M, Saikawa S, Nakamura S, Higa T, Davison KJ, Marsala M, Sugahara K (2007) Intravenous infusion of dexmedetomidine can prevent the degeneration of spinal ventral neurons induced by intrathecal morphine after a noninjurious interval of spinal cord ischemia in rats. Anesth Analg 105:1086–1093.
Kao S-C, Zhao X, Lee C-Y, Atianjoh FE, Gauda EB, Yaster M, Tao Y-X (2012) Absence of mu opioid receptor mRNA expression in astrocytes and microglia of rat spinal cord. NeuroReport 23:378–384.
Kaushal V, Koeberle PD, Wang Y, Schlichter LC (2007) The Ca2+-activated K+ channel KCNN4/KCa3.1 contributes to microglia activation and nitric oxide-dependent neurodegeneration. J Neurosci 27:234–244.
Kobayashi M, Konishi H, Sayo A, Takai T, Kiyama H (2016) TREM2/DAP12 signal elicits proinflammatory response in microglia and exacerbates neuropathic pain. J Neurosci 36:11138–11150.
Latour S, Tanaka H, Demeure C, Mateo V, Rubio M, Brown EJ, Maliszewski C, Lindberg FP, Oldenborg A, Ullrich A, Delespesse G, Sarfati M (2001) Bidirectional negative regulation of human T and dendritic cells by CD47 and its cognate receptor signal-regulator protein-alpha: down-regulation of IL-12 responsiveness and inhibition of dendritic cell activation. J Immunol 167:2547–2554.
Li Z, Wei H, Piirainen S, Chen Z, Kalso E, Pertovaara A, Tian L (2016) Spinal versus brain microglial and macrophage activation traits determine the differential neuroinflammatory responses and analgesic effect of minocycline in chronic neuropathic pain. Brain Behav Immun 58:107–117.
Loggia ML, Chonde DB, Akeju O, Arabasz G, Catana C, Edwards RR, Hill E, Hsu S, Izquierdo-Garcia D, Ji R-R, Riley M, Wasan AD, Zurcher NR, Albrecht DS, Vangel MG, Rosen BR, Napadow V, Hooker JM (2015) Evidence for brain glial activation in chronic pain patients. Brain 138:604–615.
Luo X-G, Chen S-D (2012) The changing phenotype of microglia from homeostasis to disease. Transl Neurodegener 1:9.
Maegawa H, Morimoto Y, Kudo C, Hanamoto H, Boku A, Sugimura M, Kato T, Yoshida A, Niwa H (2015) Neural mechanism underlying hyperalgesic response to orofacial pain in Parkinson's disease model rats. Neurosci Res 96:59–68.
Maiaru M, Tochiki KK, Cox MB, Annan LV, Bell CG, Feng X, Hausch F, Geranton SM (2016) The stress regulator FKBP51 drives chronic pain by modulating spinal glucocorticoid signaling. Sci Transl Med 8:325ra19.
Mattioli T-AM, Milne B, Cahill CM (2010) Ultra-low dose naltrexone attenuates chronic morphine-induced gliosis in rats. Mol Pain 6:22.
Mattioli T-AM, Leduc-Pessah H, Skelhorne-Gross G, Nicol CJB, Milne B, Trang T, Cahill CM (2014) Toll-Like, Receptor 4 Mutant and Null Mice Retain Morphine-Induced Tolerance, Hyperalgesia, and Physical Dependence. PLoS One 9(5):e97361.
Melik Parsadaniantz S, Rivat C, Rostene W, Reaux-Le Goazigo A (2015) Opioid and chemokine receptor crosstalk: a promising target for pain therapy? Nat Rev Neurosci 16:69–78.
Melzer P, Zhang MZ, McKanna JA (1997) Infraorbital nerve transection and whisker follicle removal in adult rats affect microglia and astrocytes in the trigeminal brainstem. A study with lipocortin1- and S100beta-immunohistochemistry. Neuroscience 80:459–472.
Mercadante S (1998) Pathophysiology and treatment of opioid-related myoclonus in cancer patients. Pain 74:5–9.
Obata H, Eisenach JC, Hussain H, Bynum T, Vincler M (2006) Spinal glial activation contributes to postoperative mechanical hypersensitivity in the rat. J Pain 7:816–822.
Paxinos G, Watson C (1998) The rat brain in stereotaxic coordinates. 4th ed. San Diego (USA): Academic Press.
Penttinen A-M, Suleymanova I, Albert K, Anttila J, Voutilainen MH, Airavaara M (2016) Characterization of a new low-dose 6-hydroxydopamine model of Parkinson's disease in rat. J Neurosci Res 94:318–328.
Popiolek-Barczyk K, Kolosowska N, Piotrowska A, Makuch W, Rojewska E, Jurga AM, Pilat D, Mika J (2015) Parthenolide relieves pain and promotes M2 microglia/macrophage polarization in rat model of neuropathy. Neural Plast 2015:676473.
Powell KJ, Ma W, Sutak M, Doods H, Quirion R, Jhamandas K (2000) Blockade and reversal of spinal morphine tolerance by peptide and non-peptide calcitonin gene-related peptide receptor antagonists. Br J Pharmacol 131:875–884.

Raghavendra V, Rutkowski MD, DeLeo JA (2002) The role of spinal neuroimmune activation in morphine tolerance/hyperalgesia in neuropathic and sham-operated rats. J Neurosci 22:9980–9989.
Raghavendra V, Tanga F, DeLeo JA (2003) Inhibition of microglial activation attenuates the development but not existing hypersensitivity in a rat model of neuropathy. J Pharmacol Exp Ther 306:624–630.
Ransohoff R (2016) A polarizing question: do M1 and M2 microglia exist? Nat. Neurosci 19:987–991.
Reddington M, Priller J, Treichel J, Haas C, Kreutzberg GW (1995) Astrocytes and microglia as potential targets for calcitonin gene related peptide in the central nervous system. Can J Physiol Pharmacol 73:1047–1049.
Tang Y, Le W (2016) Differential Roles of M1 and M2 Microglia in Neurodegenerative Diseases. Mol Neurobiol 53:1181–1194.
Taylor AMW, Castonguay A, Ghogha A, Vayssiere P, Pradhan AAA, Xue L, Mehrabani S, Wu J, Levitt P, Olmstead MC, De Koninck Y, Evans CJ, Cahill CM (2016) Neuroimmune regulation of GABAergic neurons within the ventral tegmental area during withdrawal from chronic morphine. Neuropsychopharmacology 41:949–959.
Tompkins DA, Campbell CM (2011) Opioid-induced hyperalgesia: clinically relevant or extraneous research phenomenon? Curr Pain Headache Rep 15:129–136.
Veinante P, Yalcin I, Barrot M (2013) The amygdala between sensation and affect: a role in pain. J Mol Psychiatry:1.
Wang Z, Ma W, Chabot J-G, Quirion R (2010) Morphological evidence for the involvement of microglial p38 activation in CGRP-associated development of morphine antinociceptive tolerance. Peptides 31:2179–2184.
Watkins LR, Hutchinson MR, Johnston IN, Maier SF (2005) Glia: novel counter-regulators of opioid analgesia. Trends Neurosci 28:661–669.
Watkins LR, Hutchinson MR, Rice KC, Maier SF (2009) The ‘‘toll” of opioid-induced glial activation: improving the clinical efficacy of opioids by targeting glia. Trends Pharmacol Sci 30:581–591.
Zhang R-X, Liu B, Wang L, Ren K, Qiao J-T, Berman BM, Lao L (2005) Spinal glial activation in a new rat model of bone cancer pain produced by prostate cancer cell inoculation of the tibia. Pain 118:125–136.
Zhang X-Q, Cui Y, Cui Y, Chen Y, Na X-D, Chen F-Y, Wei X-H, Li Y-Y, Liu X-G, Xin W-J (2012) Activation of p38 signaling in the microglia in the nucleus accumbens contributes to the acquisition and maintenance of morphine-induced conditioned place preference. Brain Behav Immun 26:318–325.
Zhu J, Qu C, Lu X, Zhang S (2014) Activation of microglia by histamine and substance P. Cell Physiol Biochem 34:768–780.
Zhuang Z-Y, Wen Y-R, Zhang D-R, Borsello T, Bonny C, Strichartz GR, Decosterd I, Ji R-R (2006) A peptide c-Jun N-terminal kinase (JNK) inhibitor blocks mechanical allodynia after spinal nerve ligation: respective roles of JNK activation in primary sensory neurons and spinal astrocytes for neuropathic pain development and maintenance. J Neurosci 26:3551–3560.
Zimmermann M (1983) Ethical guidelines for investigations of experimental pain in conscious animals. Pain 16:109–110.

(Received 29 August 2017, Accepted 23 January 2018)
(Available online 6 February 2018)